Lab on a Chip

RSC Publishing

PAPER

View Article Online
View Journal | View Issue

Cite this: *Lab Chip*, 2013, **13**, 2773

Simple replica micromolding of biocompatible styrenic elastomers†

Mark D. Borysiak,[a] Kevin S. Bielawski,[b] Nathan J. Sniadecki,[bc] Colin F. Jenkel,[b] Bryan D. Vogt[d] and Jonathan D. Posner*[ab]

Received 5th April 2013,
Accepted 25th April 2013

DOI: 10.1039/c3lc50426c

www.rsc.org/loc

In this work, we introduce a simple solvent-assisted micromolding technique for the fabrication of high-fidelity styrene-ethylene/butylene-styrene (SEBS) microfluidic devices with high polystyrene (PS) content (42 wt% PS, SEBS42). SEBS triblock copolymers are styrenic thermoplastic elastomers that exhibit both glassy thermoplastic and elastomeric properties resulting from their respective hard PS and rubbery ethylene/butylene segments. The PS fraction gives SEBS microdevices many of the appealing properties of pure PS devices, while the elastomeric properties simplify fabrication of the devices, similar to PDMS. SEBS42 devices have wettable, stable surfaces (both contact angle and zeta potential) that support cell attachment and proliferation consistent with tissue culture dish substrates, do not adsorb hydrophobic molecules, and have high bond strength to wide range of substrates (glass, PS, SEBS). Furthermore, SEBS42 devices are mechanically robust, thermally stable, as well as exhibit low auto-fluorescence and high transmissivity. We characterize SEBS42 surface properties by contact angle measurements, cell culture studies, zeta potential measurements, and the adsorption of hydrophobic molecules. The PS surface composition of SEBS microdevices cast on different substrates is determined by time-of-flight secondary ion mass spectrometry (ToF-SIMS). The attractive SEBS42 material properties, coupled with the simple fabrication method, make SEBS42 a quality substrate for microfluidic applications where the properties of PS are desired but the ease of PDMS micromolding is favoured.

Introduction

Lab-on-a-chip (LOC) devices are important tools for cellular biology research. LOC devices offer advantages over traditional macro-scale experiments due to the decreased physical scale of the systems and the resultant control of the cellular environment.[1,2] Specifically, microscale systems offer unprecedented control of the cellular microenvironment at physically relevant length and time scales associated with cellular functions and cell-based applications.[3,4] These systems offer great potential in a number of applications including drug discovery, the understanding of complex cell-cell interactions, biomechanical studies, and medical diagnostics.[5–10] Despite recent advancements, the full impact of microfluidics on cellular biology studies has not yet been realized, in part because there is often compromise in device material selection with respect to the specific research questions under consideration.[11] There is currently no material with ideal properties for cellular biology microfluidic applications, including: simple microfabrication routes, low cost, chemical stability, and biocompatibility, among others.

Traditionally, polystyrene (PS) has been the material of choice for cellular biology research, comprising the majority of tissue culture plasticware.[12] PS has many advantages when it comes to biological and chemical applications including low cost, optical transparency, biocompatibility, low auto-fluorescence, chemical stability, and facile surface functionalization. When it comes to microfluidic applications however, microfabrication of hard, glassy thermoplastic materials, such as PS, have proven to be considerably more challenging when compared to elastomeric materials such as poly-dimethylsiloxane (PDMS). Elastomeric polymers can easily replicate microstructures utilizing soft lithographic methods, resulting in their widespread use and commercialization in rapid prototyping of LOC devices.[13–15] Hard thermoplastics such as PS have traditionally relied on techniques such as injection molding and hot embossing for the replication of microstructures.[11,16–18] Injection molding is reliable and low-cost for high-volume production, but is often not practical for rapid prototyping of designs in academic labs. In the past, hot embossing has required hot-presses and expensive machined master molds that can withstand the high temperature and

[a]*Department of Chemical Engineering, University of Washington, Seattle, WA 98195, USA. E-mail: jposner@uw.edu*
[b]*Department of Mechanical Engineering, University of Washington, Seattle, WA 98195, USA*
[c]*Department of Bioengineering, University of Washington, Seattle, WA 98195, USA*
[d]*Department of Polymer Engineering, University of Akron, Akron, OH 44325, USA*
† Electronic supplementary information (ESI) available. See DOI: 10.1039/c3lc50426c

pressures associated with hot embossing procedures, making them less than ideal for rapid prototyping of LOC devices. Recently, methods have been developed that employ soft lithographic methods for replication of microstructures in hard thermoplastics, such as solvent casting on compliant PDMS molds and using negative relief PDMS molds to create low-cost, high strength epoxy molds for hot embossing.[19,20] These techniques may alleviate some of the bottlenecks associated with microstructure replication, but challenges of convenient methods for bonding and difficulties in interfacing the microfluidic network with external equipment still remain. While PDMS can reversibly or irreversibly (with use of surface treatment such as oxygen plasma) conform and seal to substrates such as glass or other pieces of PDMS, PS and hard thermoplastics require more challenging methods such as thermal pressing and solvent bonding in order to create uniform interfacial contact with other substrates. Maintaining feature fidelity becomes a concern during both thermal and solvent bonding, as PS begins to deform considerably below its glass transition temperature and solvent bonding changes the surface structure and geometry.[21] Creating access ports in thermoplastics can be time-consuming, requiring the use of manual drilling. In the more compliant PDMS, access ports can be manually punched or directly integrated during molding, allowing for simplified interfacing with external equipment.

Despite the numerous advantages of PDMS during the fabrication stage, it does have intrinsic limitations during use in LOC experiments, particularly for cell-based studies. The diffusion of small hydrophobic molecules into the PDMS bulk can significantly impact protein activation and drug discovery experiments, as well as create bias error and background noise for quantitative fluorescence measurements.[22–25] PDMS also contains uncross-linked oligomers that are able to move throughout the PDMS bulk and may leach into microfluidic solutions during experiments, potentially affecting cell membrane studies.[23] Other issues with PDMS involve its surface properties and high gas solubility.[26,27] The surface of PDMS is highly hydrophobic and often requires surface treatment to render it hydrophilic for applications such as electrophoretic separations and bioassays.[28] Oxygen plasma treatment is commonly employed, but the hydrophobic recovery in PDMS is very fast, often times occurring within hours if left in open air.[29] High gas permeability has been cited as an advantage for cell culture studies in PDMS, but it can also potentially create a hyperoxic environment that is toxic to cells.[11,30] The high permeability to water vapor often leads to changes in concentration and osmolality of microfluidic solutions during experiment, affecting cell culture conditions and assay readouts.[19,31,32] The high gas solubility combined with the unstable surface properties – particularly post-oxidation hydrophobic recovery – can result in difficulty filling channels and spontaneous formation of bubbles in microchannels, adversely affecting experimental outcomes. As a result, it is common practice to use the devices under external pressure (*e.g.* pressure reservoirs or syringe pumps), or to use the devices promptly after oxygen plasma treatment, which is not a long-term practical solution for applications. Effort has been made to chemically modify the surface to alleviate these issues, but requires additional steps and introduces new complexities.[28,33–35]

It is desirable for microfluidic devices to combine the favorable properties of PS as well as benefitting from ease of replication and fabrication processes of elastomeric materials such as PDMS.[11] One particularly viable candidate is styrene-ethylene/butylene-styrene (SEBS) block copolymers with high PS content. SEBS block copolymers are hybrid materials that exhibit both hard thermoplastic properties, as well as elastomeric properties resulting from the glassy PS blocks and the rubbery ethylene/butylene chains respectively. SEBS block copolymers are tough, inexpensive, and biocompatible materials.[36] Sudarsan *et al.* demonstrated the use of SEBS to create microfluidic networks by synthesizing melt processable elastomer gels consisting of 9 to 33 wt% SEBS mixed with mineral oil.[37] The mineral oil selectively dissolves the ethylene/butylene chains during vacuum heating to create gels that can be melt-processed to fabricate intricate, multi-layer microfluidic structures. Roy *et al.* introduced an embossing method at atmospheric pressure to quickly ($<$10 min) produce microstructures in extruded SEBS films that have been used to study cell orientation and to create a 3D microfluidic immobilization device.[36,38–40] Their method has focused on low PS content SEBS (10–15 wt% PS) and requires a twin-screw extruder in order to create the films. Overall, these works have demonstrated the versatility and potential of SEBS copolymers for use in microfluidic application.

In this work, we provide a rapid micromolding technique and thorough characterization of SEBS microfluidic devices that are a compelling alternative to PDMS, glass, and PS devices due to their simple fabrication and desirable surface and material properties. These SEBS devices have 42 wt% PS (SEBS42) and are as simple to fabricate as PDMS with many of the appealing properties of glass and PS devices. The PS material properties result from high PS content at the surface and in the bulk, while retaining elastomeric properties that simplify the molding, bonding, and connection process. SEBS42 devices have wettable, stable surfaces (both contact angle and zeta potential) that support cell attachment and proliferation consistent with tissue culture dish substrates, do not adsorb hydrophobic molecules, and have high bond strength to wide range of substrates (glass, PS, SEBS). Furthermore, SEBS42 devices are mechanically robust, thermally stable, as well as exhibit low auto-fluorescence and high transmissivity. Our characterization of SEBS42 includes the PS surface composition, contact angle measurements, zeta potential, cell culture growth, UV-vis and autofluorescence spectra, hydrophobic molecule sorption, elastic modulus, bonding strength, and thermal stability. These material properties, coupled with the simple fabrication method, make SEBS42 a quality substrate for microfluidic applications where the properties of glass or PS are desired but the ease of PDMS micromolding is favoured.

Materials and methods

Materials

SEBS block copolymers (Kraton Polymer) with 42 wt% (A1536H) and 12.5 wt% (G1645M) polystyrene were utilized as polymers for molded microfluidic devices. The 42 and 12 wt% block copolymers are referred to hereafter as SEBS42 and SEBS12, respectively. Toluene (99.8%, CAS# 108-88-3), rhodamine B (95%, CAS# 81-88-3), trichloro(1*H*,1*H*,2*H*,2*H*-perfluorooctyl)silane (97%, CAS# 78560-45-9), polystyrene (avg. M_w ~192 000), trichloro(phenethyl)silane (95%, CAS# 940-41-0), 1,2,4-trimethylbenzene (98%, CAS# 95-63-6), potassium phosphate monobasic (>99%, CAS# 7778-77-0) and sodium phosphate dibasic (>99%, CAS# 7558-79-4) were obtained from Sigma Aldrich (St. Louis, MO) and used as received. For the cell growth studies, we used human fibronectin solution (BD Biosciences), high glucose Dulbecco's modified Eagle's medium (SH30022.01, Thermo Scientific), 10% fetal bovine serum SH3981993, Thermo Scientific), and 1% penicillin-streptomycin (30-002-CI, Mediatech). SU8 2000 photoresists (MicroChem Corp, Newton, MA) and silicon wafers (Silicon Quest International, Inc., Santa Barbara, CA) were utilized to generate the master *via* photolithography. Sylgard 184 PDMS (Down Corning, Midland, MI) was used as a comparison material to SEBS and was prepared using the silicone elastomer kit.

Master mold fabrication

Three different master substrates were fabricated to investigate the effect of the substrate on the polymer surface composition: SU-8 coated, silane-treated, and untreated silicon. SU-8 coated wafers were fabricated in a two-step process so that all the surfaces in contact with the SEBS would be uniformly SU-8. First, an initial layer of photoresist 5–10 microns thick was spin-coated on a 4′′ silicon wafer and then pre-baked for 1-3 min at 95 °C. A contact aligner uniformly exposed the first SU-8 layer without a photomask. The exposed wafer was baked for 2–4 min at 95 °C. The second lithography step was standard SU-8 microstructure fabrication. An SU-8 photoresist layer 25–100 microns thick was spun on top of the initial SU-8 coating and pre-baked for 6–10 min at 95 °C. The resist was then exposed to UV-light through a printed photomask using an ABM contact aligner, baked again at 95 °C for 5–10 min, developed using Microchem SU-8 developer, and then hard-baked for 3 h at 150 °C. Positive relief micropost arrays were fabricated using SU-8 and transferred to a negative PDMS mold before SEBS casting.[41]

Molds indicated as untreated silicon were fabricated using the SU-8 coated process described above without the initial uniform SU-8 layer. Molds indicated as silane are the same as the untreated silicon with an additional trichloro(1*H*,1*H*,2*H*,2*H*-perfluorooctyl) silane treatment by vapor deposition at ambient conditions in a sealed container over night.

Replica micromolding and device fabrication

SEBS42 and SEBS12 are dissolved in toluene at 20–35 wt% solids. The high viscosity at >35 wt% solutions often result in significant surface bubble formation during casting. Following dissolution of the solid, the solutions are de-gassed under vacuum for 5–10 min before casting onto the master molds. The solution is retained on the mold using a PTFE coated metallic ring (666 ring, Norpro, Everett, WA) that surrounds the wafer. The SEBS molded sample is baked in a two-step process at 60 °C for 5 h and 95 °C for 8 h using a hotplate in a fume hood. Following baking, the SEBS is gently peeled from the mold. Surface bubbles may form during solvent evaporation with toluene. These can be reduced by sonication of the mixture for 1 min, followed by a second de-gassing for 5 min. If a lower vapor pressure solvent is desired for reduction of surface bubbles during casting, 1,2,4-trimethylbenzene (b.p. = 168 °C) can be used in place of toluene. Recommended baking conditions for 1,2,4-trimethylbenzene are 115 °C for 5 h and 145 °C for 10 h. All data presented herein utilized toluene as the casting solvent.

For bonding of SEBS to substrates such glass, PS, and other SEBS, oxygen plasma treatment and/or heating are used to ensure uniform interfacial contact. Reversible bonding to PS or other SEBS substrates is achieved by simply pressing the two substrates together or by using plasma oxidation treatment on both surfaces to be bonded with a Harrick Plasma Cleaner (PDC-001, Ithaca, NY) for 5 min at 30 W and a flow of 10 sccm O_2. For a stronger, irreversible bond, the substrates are placed into contact and baked at 75 °C for 30–60 min, followed by firmly pressing the two substrates together. Quality bonding to glass is not achievable without the use of thermal bonding. We did not observe any deformation of the microstructures when bonding thermally to PS, SEBS, or glass.

We measured the maximum pressure that SEBS42 bonded to SEBS42 could withstand with no treatment, oxygen plasma treatment, and following annealing at 75 °C. We also measured SEBS42 thermally bonded to glass and PS. Small PS cylindrical wells were attached to the SEBS surface with epoxy and filled with colored water. We pressurized the fluid using argon gas and increased the pressure until we observed fluid leaking from the channel. The connection to the devices failed at pressures greater than 60 psi.

Methods to assess SEBS properties and performance

We evaluated both the physical properties (surface composition, contact angle, zeta potential, elastic modulus, thermal stability, UV-vis transmission, and auto-fluorescence) and performance in microfluidic applications of the SEBS substrates. SEBS was also tested as a cell culture substrate and its permeability to a hydrophobic fluorescent dye was assessed. Here we describe the methods used to assess the SEBS properties and performance.

Cell culture

We prepared SEBS42 substrates for cell culture by casting on flat silicon wafers coated with a thin layer of SU-8. The four different sets of SEBS substrates were: native SEBS, SEBS treated with ozone for 7 min in a UVO Cleaner (Jelight), SEBS with human fibronectin (FN) solution (50 μg ml^{-1}, BD Biosciences) adsorbed to the surface for 1 h, and SEBS treated with ozone followed by adsorption of FN. In addition, we prepared PDMS substrates by adsorbing the same concentration of FN onto the surface. All substrates were rinsed in 100% ethanol, followed by 70% ethanol and sterile deionized water before being placed into wells of a 6-well tissue culture dish

(657160, Greiner Bio-one). Cell culture media consisting of high glucose Dulbecco's modified Eagle's medium (SH30022.01, Thermo Scientific), 10% fetal bovine serum (SH3981993, Thermo Scientific), and 1% penicillin-streptomycin (30-002-CI, Mediatech) were added to each well and incubated for 20 min prior to seeding mouse 3T3 fibroblast cells (NIH 3T3 fibroblasts, from C. Chen, University of Pennsylvania) or bovine pulmonary arterial endothelial cells (BPAECs, BW-6004, Lonza) onto the substrates. Media was exchanged on days 2, 4, and 6.

On days 2, 4, 6, and 9, a group of substrates were removed from the incubator and the cells were fixed in a solution of 4% paraformaldehyde. The cells were permeabilized and stained using 0.2% Triton X-100 and Hoesch 33342 (H1399, Invitrogen), respectively. The cells were mounted with coverslips using Fluoromount G (0100-01, Southern Biotech) before fluorescent imaging of the cells at the center and each corner of each substrate using a Nikon Eclipse TI inverted microscope and a 10× objective. The number of cells in each image were counted using Nikon Elements analysis software.

Analyses of Variance (ANOVA) with equal replication statistical tests were used to analyze the differences in cell growth on the various substrates for day 2, 4, 6, and 9. Tukey–Kramer comparison of means tests determined the statistical differences between samples. All statistical results are reported at 95% confidence intervals ($\alpha = 0.05$).

Contact angle

Advancing and receding water contact angle measurements were performed with a goniometer (Ramé-Hart Instrument Co., Netcong, NJ) using a dynamic sessile drop method on flat substrates of SEBS42, SEBS12, PDMS, and PS. The substrates were cast from flat silicon wafers coated with a thin layer of SU-8 and oxidized (Harrick Plasma Cleaner PDC-001, Ithaca, NY) for 5 min at 30 W and a flow of 10 sccm O_2 following casting. Measurements were also made on the native surface that did not receive any treatment following casting. The advancing and receding angles correspond to constant angle measurements for increasing and decreasing drop volume, respectively. Each angle measurement is the average of five drops on three different samples for both SEBS42 and SEBS12 with standard deviations reported.

Time of flight secondary ion mass spectrometry

Time of flight secondary ion mass spectrometry (TOF-SIMS) spectra of SEBS42 and SEBS12 samples were acquired on an IonTof ToF-SIMS 5-100 spectrometer using an 25 keV Bi_3^+ cluster ion source in the pulsed mode. SEBS42 and SEBS12 were cast on silicon wafers coated with a thin layer of SU-8, silicon wafers treated with silane, and untreated silicon wafers. Small square samples (1 mm × 1 mm) were prepared and rinsed thoroughly with isopropyl alcohol, ethanol, and DI water. ToF-SIMS spectra were acquired for both positive and negative secondary ions over a mass range of $m/z = 0$ to 700. The ion source was operated at a current of 0.14 pA. The secondary ion dose was kept below 5×10^{11} ions per cm^2. Secondary ions of a given polarity were extracted and detected using a reflectron time-of-flight mass analyzer. Spectra were acquired using an analysis area of 100 × 100 μm. Positive ion spectra were calibrated using the CH_3^+, $C_2H_3^+$, $C_3H_5^+$, and $C_8H_7^+$ peaks. The negative ion spectra were calibrated using the CH^-, OH^-, C_2H^- peaks. Calibration errors were kept below 10 ppm. Mass resolution ($m/\Delta m$) for a typical spectrum was 4500 to 5200 for $m/z = 27$ (positive) and 5500 to 6500 for $m/z = 25$ (negative).

Dye adsorption and absorption

Simple dye adsorption and absorption measurements for SEBS42 and PDMS devices were performed with microfluidic channels (50 μm width, 30 μm depth) filled with 100 μM rhodamine B (81-88-3, Sigma Aldrich, St. Louis, MO) solution for 15 min and 24 h. An inverted epi-fluorescence microscope (Nikon TE2000, Melville, NY), a fluorescent optical filter set (XF108-2, Omega, Brattleboro, VT), 10× objective, and cooled digital camera (Cascade IIb, Photometrics, Tucson, AZ) imaged the rhodamine dye in the microchannel after 15 min and 24 h. The channels were thoroughly rinsed with DI water and re-imaged to observe dye adsorption.

Optical properties

The 1 mm thick, 1″ × 1″ sample substrate's transmissibility was determined using a UV/vis/NIR spectrometer (Lambda 1050, PerkinElmer, Waltham, MA) equipped with an integrating sphere. The auto-fluorescence of SEBS42 formed to the shape of a standard 3.5 mL cuvette was determined using a luminescence spectrometer (LS55, PerkinElmer, Waltham, MA). The samples were excited from 200–800 nm in 10 nm intervals, while recording emission scans from 200–800 nm for each excitation wavelength. The SEBS42 is compared to the spectra of a polystyrene fluorometer cuvette (cat# 9012, Perfector Science, Atascadero, CA) with the same experimental setup.

Mechanical properties

The mechanical testing was conducted according to the ASTM standard D638-10. 1–1.5 mm thick SEBS samples were molded according to Type IV dimensions, with a gauge length and thickness of 25 mm and 6 mm respectively. The tensile tests were performed using an Instron high load frame (5585H, Instron, Los Angeles, CA) at a speed of 2 mm min^{-1} under ambient conditions. The stress-strain curves were recorded using a static axial extensometer (cat# 2630-106, Instron, Los Angeles, CA) for a minimum of five replicates for each sample. The modulus of elasticity is reported as the linear response of the stress-strain curve.

Thermal stability

Differential scanning calorimetry measurements were made on three SEBS42 samples using a Q2000 DSC (TA Instruments) at constant heating of 5 °C min^{-1}. Additionally, 50 μm-wide microchannels were heated on a hotplate from 30–180 °C with constant fluid flow. The channels were optically monitored for deformation due to softening from increased temperatures.

Zeta potential measurements

We measured the zeta potential of SEBS42 using current monitoring experiments.[42] Microchannels 200 μm wide, 50 μm tall, and 4 cm in length were fabricated by casting on all SU-8

wafers. The microchannels ports were punched using a syringe needle, thermally bonded at 75 °C to a flat SEBS substrate, and PS cylinder wells were attached using UV-curable epoxy. Stock 100 mM phosphate buffer solution was prepared at 22 °C by mixing equimolar sodium phosphate dibasic and sodium phosphate monobasic in DI water before dilution to 9.5 and 10 mM concentration. The bulk conductivities of the phosphate solutions were measured using a high-precision conductivity meter. The 9.5 mM phosphate solution measured λ_b = 1346 μS cm^{-1} and the 10 mM phosphate solution measured λ_b = 1285 μS cm^{-1}. The diluted samples had a pH of 6.92, measured at 22 °C. Multiple measurements were made on at least three microdevices from different batches over the course of multiple weeks at a temperature of 22.0 ± 0.5 °C.

The channel was thoroughly washed with 100 mM NaOH, DI water, and 9.5 mM phosphate buffer solution before monitoring. Both wells and the channel were filled with 9.5 mM phosphate buffer solution using a syringe with a 0.2 micron filter and a potential difference of 200 V was applied *via* platinum electrodes placed into each well using a remote source meter (Keithley 6430, Cleveland, OH) until a constant current was observed. One channel was then cleared with vacuum and injected with 10 mM phosphate solution through using a syringe with a 0.2 micron filter. A 200 V potential difference was applied and the change in current with respect to time was monitored using source meter and recorded using Labview. The zeta potential was calculated using the slope of the current-time plot and the Smoluchowski equation, as previously reported by Sze *et al.* (see ESI†).[42]

Results and discussion

Device fabrication

Microstructures are replicated by pouring dissolved SEBS onto an SU-8 master mold, followed by a two-step baking process. The amount of solution added is dependent upon the desired thickness of the microdevices, with micromolds ranging from ~0.1 mm to 5 mm thick easily fabricated. The initial low temperature baking step at 60 °C is to remove a majority of the solvent well below the boiling point of toluene (110.6 °C), while the second step at 95 °C ensures complete removal of the solvent. We are able to reproduce high fidelity microstructures with this molding process.

Fig. 1 illustrates replication of 50 μm wide microchannels and microposts with a 4 : 1 aspect ratio and 7 μm spacing. Microstructures as small as 2 μm have been successfully replicated in SEBS. The minimum feature size is currently limited by the minimum resolution of the SU-8 master mold. The compliance of the SEBS allows it to be easily peeled from rigid mold surfaces during de-molding, while maintaining feature integrity.

Silane treatment of the master mold assists in release of the SEBS and preserves the microstructures during repeated castings, although the silane impacts the SEBS device surface composition, as will be discussed later. Casting on a silicon wafer with SU-8 microstructures and no surface treatment leads to difficulty in removing the SEBS from the mold and resultant microstructure damage as early as the initial casting. Applying a thin coating of SU-8 to the silicon wafer before fabricating the microstructures however, results in a stronger adhesion of SU-8 microstructures and provides improved release in comparison to SU-8 on untreated silicon wafers. This route also produces more PS surface functionality than silane treated wafers. In our hands, silane treated wafers could be used >25 times on average without any noticeable defects, while all SU-8 wafers could be used >15 times on average.

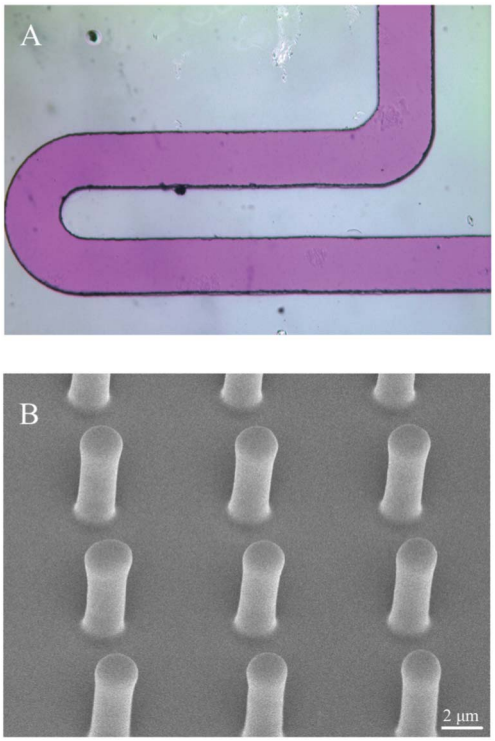

Fig. 1 Image A shows 50 μm wide microchannel filled with dye. Image B shows an SEM image of 8 × 2 μm (height × diameter) microposts with 7 μm spacing at 40° tilt molded in SEBS42, demonstrating the high fidelity replication.

Bonding and access port interfacing is easily achieved in SEBS materials with rounded punches similar to protocols for PDMS. This methodology greatly simplifies the fabrication process when compared to hard thermoplastics. Molded SEBS can be reversibly or irreversibly bonded to a number of substrates including PS, SEBS, and glass. Reversible bonding of SEBS to PS or SEBS is facilitated by oxygen plasma treatment of the two surfaces to be bonded, but simply firmly pressing the two substrates together at room temperature without treatment provides some bonding; however, this is weaker than the plasma bond. Irreversible bonding can be achieved through heating at 75 °C while the surfaces are in intimate contact, followed by manual pressure. Effective bonding to glass is only possible with this thermal treatment.

Devices of SEBS42 reversibly bonded to SEBS42 were able to withstand 20–30 psi of pressure without oxygen plasma treatment and 30–35 psi of pressure with oxygen plasma treatment before leakage due to delamination. Devices of SEBS42 irreversibly bonded to SEBS42, PS, and glass at 75 °C for 30 min did not rupture or delaminate when we applied 60

psi of pressure to the filled channel. This suggests that reversible bonding of SEBS42 can facilitate passive and low-pressure fluid flows, while the irreversible bonding is satisfactory for the majority of applications requiring pressure driven flows. We can achieve an irreversible bond with or without plasma treatment, allowing for pressure driven flow with the native or oxidized surface. Typical PDMS-glass bonds range from 30–50 psi, with as high as 70 psi reported.[43,44]

Mechanical and thermal properties

We determined the modulus of elasticity of SEBS42 and SEBS12 to be 6.18 $\pm$ 0.29 MPa and 0.86 $\pm$ 0.12 MPa respectively (see Table S1, ESI† for additional mechanical properties). The increase in PS content in SEBS42 results in a stiffness 2–6$\times$ greater than standard 10 : 1 ratio Sylgard 184 PDMS and SEBS with 10–15 wt% PS.[39,45] SEBS42 and SEBS with large PS content in general are intriguing materials for potential sub-micron resolution molds and stamps. Standard Sylgard 184 PDMS formulations often experience structure collapse with decreasing sub-micron structures due to its low modulus and high free volume matrix structure.[45–47] The increased toughness and hardness of SEBS42 in comparison to PDMS or previously investigated SEBS indicate that it may be well-suited for these applications.[47,48] Furthermore, SEBS with high polystyrene content and increased stiffness should be well suited for studies that require dimensional stability.[19,43] Optimally, SEBS stiffness and hardness could be manipulated for specific applications with the use of the wide variety of commercially available SEBS and the blending of multiple formulations if necessary. We are currently developing blends of SEBS with 67 wt% PS that exhibit a wide range of material stiffness and elastomeric behaviors.

We studied the thermal stability of the SEBS by differential scanning calorimetry (DSC) and observation of fluid flow through a microchannel on a hotplate with increasing temperature. The results from these two experiments indicate that SEBS42 has relatively high thermal stability at temperatures of experimental interest, *e.g.* 95 °C for PCR applications. The glass transition of SEBS is typically in the range of 80–90 °C;[39,49] however, we have found during our experiments that this transition is very mild and does not have a noticeable effect on device function. The DSC results (see ESI†, Fig. S9) do not show large fluctuations that are typically seen for significant phase transitions. This is not surprising, as SEBS polymers are commonly employed in applications where high-servicing temperature and processing stability are required. This behavior is in contrast to pure PS which significantly deforms at temperatures near its glass transition temperature of 90–95 °C.[49] The DSC results were confirmed by observing flow through a SEBS42 microchannel at elevated temperatures. At 95 °C, no deformation of the channels was observed due to softening of the polymer.

The thermal conductivity of SEBS is approximately 0.46–0.66 W m^{-1} K^{-1}.[49,50] This thermal conductivity is consistent with common polymers such as PS, PDMS, PMMA, acrylic, *etc*. A low thermal conductivity has both drawbacks and advantages for microfluidic use. The low conductivity value results in a reduced dissipation of heat from the microchannel. For electrokinetic applications, this may result in Joule heating in the channel. However, for applications such as PCR on a chip, this thermal stability may help to maintain a consistent reaction temperature with a lower heating load, provided that the heating elements are incorporated into the chip or the sealing substrate is a higher thermal conductivity material. Additionally, the low thermal conductivity may provide a stable thermal environment for the incubation of cells.

Surface composition

The polymer surface provides the interface that controls interaction between the microstructures and the biological or solution environment. The physical and chemical interactions based upon the first few nanometers near the polymer surface determine properties such as adhesion, wetting, and electrochemical properties and dictate many practical applications. For biological microfluidic applications with SEBS, we believe it is desirable for micromolded SEBS to maximize the PS content at the microstructure surface. PS exhibits a more hydrophilic surface than PEB and has repeatedly proven to be a material well-suited for biological applications.[11] Preferential wetting of one segment of the block copolymer at the surface is predominantly controlled by the relative surface energies,[51–54] but here the wetting at the master substrate interface controls the surface presented by the molded SEBS microstructure.[55] The composition of the polymer-substrate interface is dependent upon the functionality of the substrate surface and its respective interaction with the PS and PEB blocks.[52,56,57] The fraction of each block in the copolymer (and the resultant morphology) will also affect the segregation and structure of the copolymer at the surface.[58]

The surface compositions of SEBS42 and SEBS12 cast on SU-8 and silane treated surfaces and SEBS42 on untreated silicon wafers are analysed by static ToF-SIMS. Spectra of the SEBS surface peeled from the wafer are measured and recorded. We perform multivariate principle component analysis (PCA) for comparison of the different samples using the NESAC/BIO toolbox.[59] PCA is a powerful tool that utilizes the entire peak spectrum in order to identify the major sources of variance within and between samples.[59–61] It generates two important matrices: the scores, which show the relationships between the samples for a given principal component and the loadings, which specify the variables (peaks) that are responsible for the separation seen in the scores plot.

The ESI contains a detailed explanation of the ToF-SIMS analysis, with the pertinent results discussed here. Table 1 lists the scores of the PCA analysis for principal component 1. The scores are a semi-quantitative comparison of PS content, as samples with more negative scores have greater PS content at the surface than samples with more positive scores. For the same casting surface, SEBS42 exhibits more negative scores relative to SEBS12, suggesting higher surface PS content as might be expected for the larger PS content in the block copolymer. Furthermore, the data shows that more PS is present on the surface when the SEBS is cast on SU-8 compared to silane treated wafers. Casting on silicon surfaces results in the maximum amount of PS at the surface. PS is increasingly at the surface when casting on surfaces with the greater attractive forces between PS and substrate, which agree

Table 1 The scores (a.u.) and average surface concentration (PS, mol%) for SEBS42 and SEBS12 at various substrates. The scores indicate relative differences in PS at the surface, as determined by PCA analysis (see ESI). More negative scores indicate greater PS surface concentration, while more positive scores indicate greater PEB surface concentration. The average surface concentration is calculated using characteristic ion peaks and eqn (1). The results show that the fraction of PS in the bulk of the copolymer, as well as the substrate surface have a large effect on the amount of PS that segregates to the surface during casting and annealing. Pure PS cast on SU-8 is shown as a reference. Errors in parentheses indicate 95% confidence intervals

Surface	Polymer	Score	Average surface concentration
SU-8	SEBS42	−6.7 (±1.3)	25.5 (±8.1)
	SEBS12	28.9 (±1.7)	3.74 (±1.21)
	PS	−39.8 (±2.1)	85.9 (±5.1)
Silane	SEBS42	0.34 (±0.58)	15.9 (±6.5)
	SEBS12	31.0 (±3.5)	2.38 (±0.76)
Silicon	SEBS42	−13.7 (±0.46)	36.6 (±9.4)

qualitatively with work of adhesion calculations (see ESI†, Table S3).

The results of the PCA analysis can be compared to quantitative calculations using characteristic ion peaks. Quantitative analysis of block copolymer segregation to interfaces has been reported previously using the relative intensity of characteristic ion peaks to quantify molar surface composition.[62–64] The molar fraction of PS at the surface can be defined by,

$$R = \frac{I_{PS}}{I_{PS} + I_{PEB}} \quad (1)$$

where I_{PS} and I_{PEB} are the total intensities of the characteristic ions from PS and PEB respectively.[62,63] Table 1 shows the molar fraction of PS at the surface for SEBS42 and SEBS12 at the various substrate surfaces. The peaks chosen to calculate the fractions in Table 1 are the characteristic peaks for each polymer block that we believe to be least affected by matrix effects (see ESI†).[62] SEBS42 cast on SU-8 has approximately 25% PS at the surface, while SEBS12 cast on SU-8 has approximately 4% PS at the surface. SEBS42 cast on silane has approximately 15% PS at the surface, while SEBS12 cast on silane has less than 2% PS at the surface. SEBS42 cast on silicon results in the maximum amount of PS with 36% PS at the surface. The large 95% confidence intervals indicate the uncertainty of the quantitative results, but overall, the trends match up very well with the PCA results that utilize the entire spectrum and are much less sensitive to matrix effects.

Collectively, the SIMS results indicate that the surface-polymer interactions, as well as the fraction of PS in the copolymer affect the amount of PS at the surface. SEBS42 has significantly more PS at the surface than SEBS12 on all surfaces. Silicon casting substrates result in the most PS at the surface, followed by SU-8 and then silane surfaces. However, the trade-off with practical usefulness in regards to master mold integrity (*i.e.* silane molds experience very little degradation and silicon molds result in microstructure removal) must also be considered. Other master substrate surface treatments are available as well. For instance, we have found that trichloro(phenethyl)silane produces a highly durable wafer surface with a surface composition likely similar to SU-8 based on work of adhesion calculations (see ESI†, Table S3).

Surface properties

The native surface of both SEBS42 and SEBS12 cast on SU-8 are hydrophobic, exhibiting advancing water contact angles greater than 90°. The advancing angles for SEBS42 and SEBS12 are 95.9° ± 2.3° and 113.0 ± 1.8° respectively, while the receding angles are 71.0 ± 2.5° and 73.7° ± 2.1°. PS has an advancing contact angle of 91–94°, while PE and PB have advancing contact angles of 97 and 112° respectively. The larger advancing contact angle for SEBS12 compared to SEBS42 can likely be attributed to a higher concentration of the more hydrophobic PEB at the surface.

Oxygen plasma treatment is often used to oxidize the native surface of polymers in order to create a more hydrophilic surface for passive flow of polar liquids such as aqueous solutions, to clean and bond the substrates, and to assist in cell attachment. PDMS has a well-known limitation of fast hydrophobic recovery following surface oxidation due to the low glass transition temperature of PDMS (−120 °C) and the resultant mobility of uncross-linked hydrophobic oligomers in the bulk that are able to migrate to the surface.[29] The advancing contact angle of native PDMS is 108°. Fig. 2 shows the rapid (<24 h) hydrophobic recovery of PDMS from an initial hydrophilic state with a contact angle of ~30° to a hydrophobic state of approximately 97–100°. We also observed high spatial variability of the recovery across the surface, which resulted in a non-uniform wetting surface. In contrast, PS presents a hydrophilic surface following plasma treatment with a much slower and less severe hydrophobic recovery from ~35° to ~50° over the course of three days with less spatial variation in the contact angle.[65] This stability gives tissue

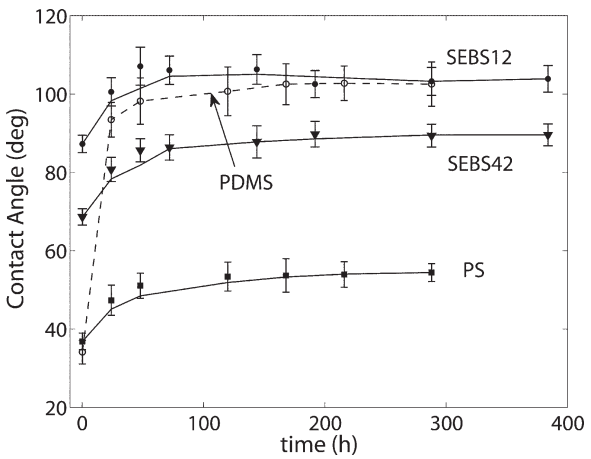

Fig. 2 Advancing contact angle measurements following oxygen plasma treatment. SEBS42 (closed triangles) has greater wettability than SEBS12 (closed circles) and exhibits a moderate hydrophobic recovery. PS (closed squares) and PDMS (open circles, dashed line) are shown for reference. The recovery of SEBS is similar to PS and mild compared to PDMS. Error bars indicate ± one standard deviation.

culture dishes that are surface-treated by manufacturers their long shelf life for supporting cell attachment.[20,65]

Following relatively mild plasma treatment of 10 sccm of O_2 at 30 W for 5 min, the SEBS surface exhibits a moderately hydrophilic surface as seen in Fig. 2. The SEBS42 surface undergoes a recovery from $\sim$70 to $\sim$85° over the course of 3–4 days with spatial variation similar to PS. SEBS42 is less hydrophilic than PS following plasma treatment and after recovery, but undergoes a similar recovery time. Compared to PDMS, SEBS42's surface is more hydrophilic and stable (*i.e.* slower recovery, smaller change in contact angle during recovery, and less spatial variation in contact angle). SEBS12 substrate recovers to a hydrophobic surface similar to PDMS as a result of limited rigid PS blocks in the bulk and at the surface. Note that higher power plasma treatment increases the degree of wetting for all substrates,[65] although we expect the recovery trends (*i.e.* recovery time and change of contact angle) to remain similar to the presented data. The wettability of SEBS42 indicates that the surface is suitable for cell attachment and passive flow of polar liquids – both important factors in biological microfluidic experiments.[66,67]

Stability of the zeta potential, a fundamental parameter of electrical double layer models, is important for substrates used in electrokinetic separation techniques and other microfluidic applications involving electroosmotic flow. The zeta potential normalized by the negative logarithm of the counterion concentration, ζ/pC,[68,69] of the native surface of SEBS42 cast on SU-8 is -39.5 ± 4.4 mV (pC = 1.824), as determined by current monitoring experiments using 9.5 and 10 mM phosphate solutions (pH = 6.92) and an applied voltage of 200 V.[42] The zeta potential is similar to typical values reported for current monitoring experiments conducted on various polymers, such as PS, PE, and PDMS.[69] More importantly, the zeta potential for SEBS42 showed consistency between devices (and batches) and for measurements made over the course of several weeks. In contrast to PDMS, SEBS42 devices can be stored in air. SEBS42 surface offers a stable, consistent surface for electrokinetic experiments with very simple device fabrication and use.

Another advantage of the SEBS42 devices relative to PDMS is the ease in filling of the channels using aqueous solutions without formation of bubbles at atmospheric conditions. Conversely, PDMS devices will often retain bubbles while filling and spontaneously form bubbles in filled channels due to its high gas permeability and hydrophobicity. For these reasons, PDMS devices are most often used promptly after plasma treatment, with chemically modified surfaces, or under sustained pressure from syringe pumps or pressure reservoirs. Water filled SEBS42 microchannels do not form bubbles in the channels when allowed to sit in open air for weeks, demonstrating that these issues are mitigated in SEBS devices.

Cell biocompatibility

Fig. 3 illustrates the growth of 3T3 (Fig. 3a) and BPAEC (Fig. 3b) cells over nine days on SEBS substrates subjected to different treatments: native surface, ozone treated, fibronectin (FN) coated, and ozone/FN. The number of cells on these substrates are directly compared with cells seeded onto tissue culture (TC) dishes and PDMS substrates coated with FN for culturing times of 2, 4, 6 and 9 days. We use comparison of means statistical testing to determine whether growth on each substrate is significantly different from the other substrates for each day. Fig. 3 shows the full results of statistical testing (α = 0.05) between substrates for each day and cell type. Peaks with the same letter do not significantly differ from each other for that day. Peaks with two letters do not significantly differ from peaks with either of the corresponding letters (*i.e.* are intermediate) on that respective day. Images of 3T3 and BPAEC cell growth on each substrate after six days of culture are found in the supplementary information, Fig. S6, ESI†. Consistency in the cell shape is observed for all the surfaces.

On TC dishes, 3T3s proliferate and reach confluence by day 4. Throughout the entire experiment, the four treatments of SEBS and PDMS showed no statistically significant difference for the 3T3 cells. As PDMS with FN treatment has been noted as a good substrate for culturing 3T3 cells, this result indicates that SEBS with any treatment is a suitable substrate for 3T3 growth.[70] On days 2 and 4, the TC dish demonstrates significantly greater growth than the SEBS and PDMS substrate. At longer growth times however, the SEBS substrates and TC dish growth are more comparable. There is no significant difference between the native, ozone treated, or FN coated SEBS and the TC dish on day 9, though this may be due in part to cell detachment following the TC dish reaching confluence early in the experiment.

The BPAEC cells are primary epithelial cells that are more sensitive to culture conditions. As shown in Fig. 3b, this sensitivity results in larger variance in cell growth between the substrates. On TC dishes, BPAEC cells reach confluence by day 9. The TC dish shows greater initial attachment than all other substrates on day 2 and the native SEBS and SEBS with ozone treatment experienced significantly less growth than the TC dish throughout the experiment. On days 4–9 however, SEBS with FN coating exhibited growth that did not significantly differ from the TC dish. In general, the PDMS demonstrated growth that was intermediate between the low growth substrates and higher growth SEBS substrates.

These results show that SEBS42 will promote cell adhesion and proliferation independent of the surface treatment. In most cases, the proliferation was comparable or exceeded the growth on PDMS substrates adsorbed with FN, a common microfluidic cell culture substrate.[70] The results also compare well to cell growth on SEBS12 substrates.[36] Our experiments also confirm that native PS surfaces and PS with FN treatment exhibit negligible cell attachment and proliferation (data not shown).[67] Interestingly, the native and FN treated SEBS42 surface is capable of cell attachment and proliferation. The proliferation on FN treated SEBS42 is comparable to standard tissue culture dish cell growth. Overall, these results demonstrate that SEBS42 is capable of promoting adhesion and proliferation of different cell lines with multiple surface treatments, enabling potential use for ''cell-culture-on-a-chip'' and other cell-based microfluidic studies.

Absorption and optical properties

PDMS has a tendency to sorb small hydrophobic molecules into its high free volume matrix.[22,70] Experiments that require

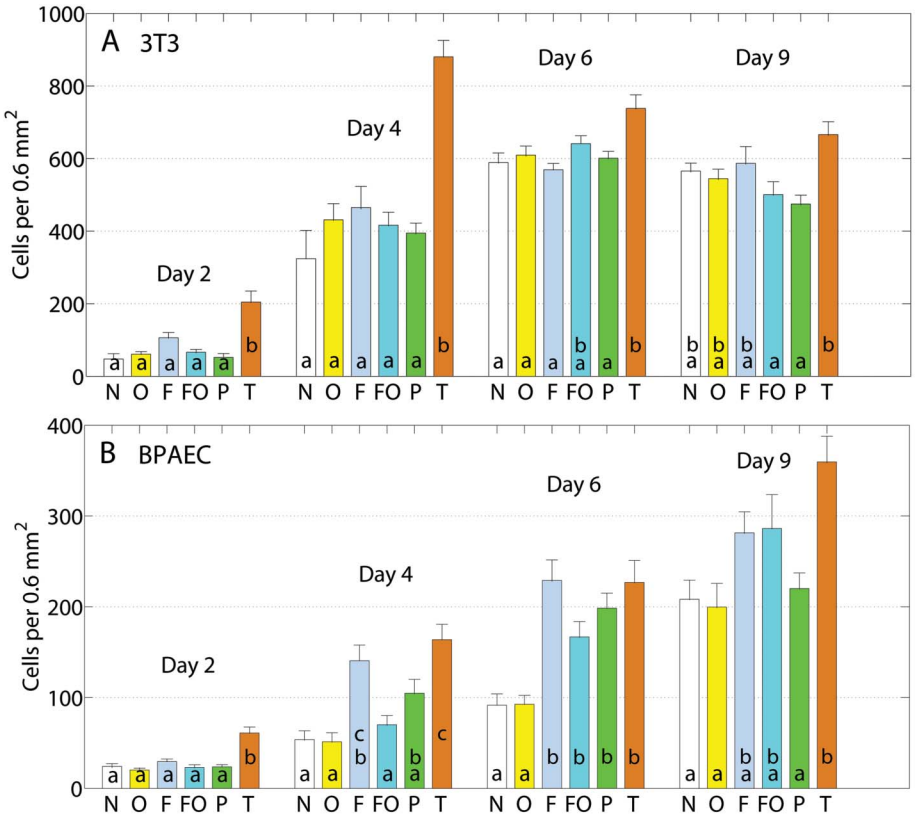

Fig. 3 3T3 (A) and BPAEC (B) cell growth on various SEBS substrates (N = native, O = ozone treatment, F = fibronectin treatment, FO = ozone/fibronectin treatment), PDMS treated with fibronectin (P), and tissue culture dishes (T) over the course of nine days. Peaks labelled with the same letter do not significantly differ from each other ($\alpha = 0.05$) on that respective day. Peaks labelled with two letters do not significantly differ from peaks with either of the corresponding letters (*i.e.* are intermediate) on that respective day. In general, the results show that 3T3 cell growth on SEBS of all treatments is similar to PDMS throughout the experiment and to the control tissue culture dish over longer periods (days 6 and 9). For BPAEC growth, SEBS treated with FN does not differ significantly from the TC dish after day 2 and in most cases, PDMS growth is similar to SEBS. The error bars indicate one standard deviation.

the use of hormones or other small molecule drugs, as well as quantitative dye studies can be challenging in PDMS microfluidic devices due to these intrinsic material properties.[23,25] For PDMS, molecule sorption can be reduced and biocompatibility can be improved using treatments such as sol–gel method or coating with paraffin or parylene,[34,71–73] but this introduces further processing steps for the fabrication of microfluidic devices simply due to material limitations.

Rhodamine B is a small amphoteric dye that is neutral from pH 6–10,[74] and demonstrates the issues associated with sorption of small hydrophobic molecules in PDMS. Fig. 4 shows 50 μm wide channels filled with 100 μM rhodamine B using native SEBS42 cast on SU-8 and native PDMS. As seen in Fig. 4b and the corresponding intensity profile (Fig. 4c), rhodamine B strongly absorbs into PDMS with significant penetration into the porous bulk. Despite thorough washing with DI water following incubation, the channel and the walls of the PDMS remain fluorescent (Fig. 4e,f) demonstrating its tendency to adsorb, as well as absorb small hydrophobic molecules. Conversely, SEBS42 does not appear to have significant absorption of rhodamine B into the bulk material (Fig. 4a,c). Following a thorough washing with DI water, the fluorescent signal of the dye in SEBS42 is essentially removed from the channel, demonstrating very weak adsorptive interactions between the dye and SEBS42 surface (Fig. 4d,f). Nearly identical results were observed after 24 h of incubation, suggesting that SEBS42 is suitable for long-term incubation typically required in cell biology experiments (see ESI†, Fig. S5). These results match well with experiments performed on pure PS and indicate that the adsorption and absorption of small hydrophobic molecules, such as rhodamine B, are highly reduced or eliminated in SEBS42.[20]

The ability to clearly image experimental progress in microfluidic chips, either through optical or fluorescent readings is an essential property for any LOC device. Fig. 5 shows the percent transmittance for SEBS42, SEBS12, PDMS, and pure PS in the UV and low-visible spectra ranges. All four polymers have similar transmittance in the high UV-visible range (400–800 nm), nearing 100% transmittance. At shorter wavelengths (200–300 nm), PDMS exhibits greater transmittance than the other polymers, with the SEBS demonstrating slightly improved transmittance over pure PS in the 200–400 nm range. Autofluorescence studies on SEBS42 also indicate that the background fluorescence of SEBS42 is low and comparable to PS cuvette standards (see ESI†, Fig. S7 and S8).

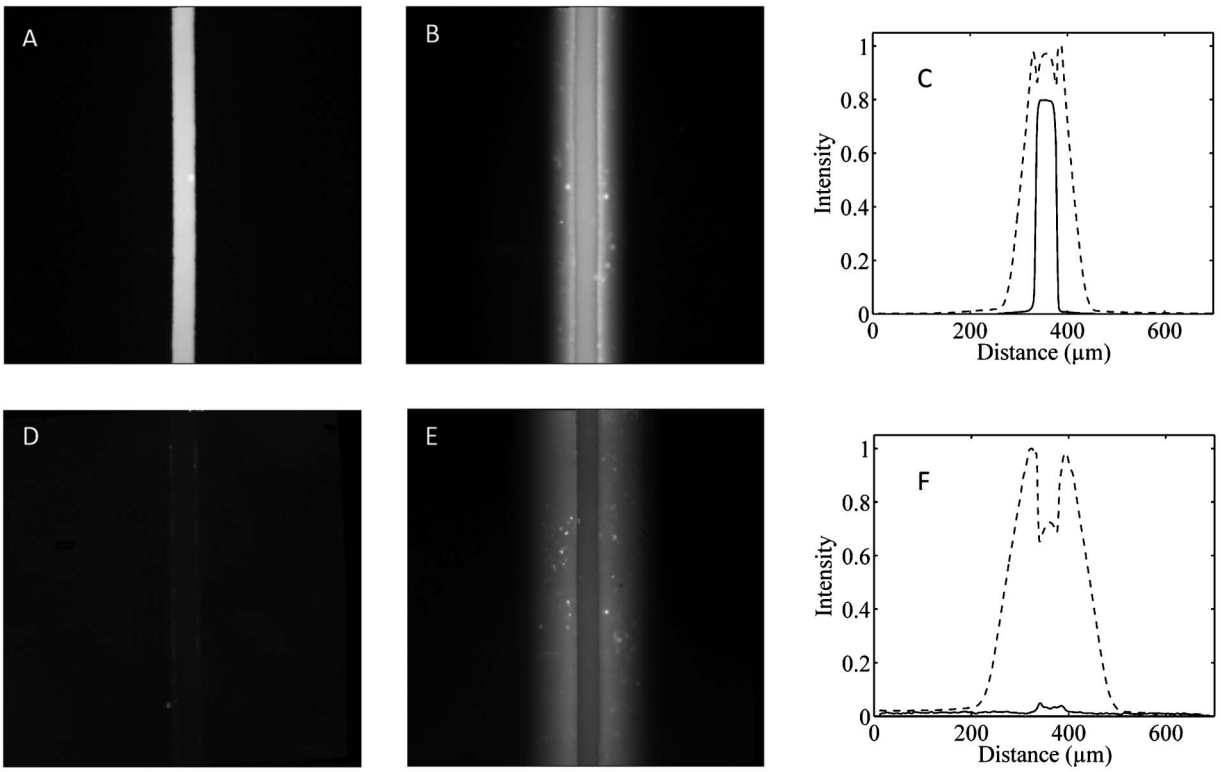

Fig. 4 Rhodamine B adsorption and absorption studies. Images A and B show the absorption of 100 μM rhodamine B (15 min incubation) in 50 μm wide channels fabricated from SEBS42 and PDMS respectively. Images D and E show SEBS42 and PDMS adsorption and leakage after thorough rinsing with DI water. The corresponding intensity profiles (C and F) show the normalized fluorescence intensity of SEBS42 (solid line) and PDMS (dashed line) for the respective images. The results demonstrate that the small hydrophobic molecule adsorption and absorption experienced in PDMS is absent in SEBS42. The intensity profiles are spatially averaged in the *y*-direction and are normalized to the overall maximum and minimum intensity in each graph.

Summary

Microfluidic devices fabricated from SEBS containing high PS content combine many of the desirable properties of PS with elastomeric properties that offer convenient methods for microfabrication. Table 2 summarizes relevant properties for SEBS12, SEBS42, PDMS, and PS. Microstructures with high resolution and fidelity are easily replicated in SEBS through a solvent-assisted replica micromolding. Toluene is a recommended solvent, but issues can arise with surface bubble formation during casting if not properly degassed. In this case, other higher BP solvents such as 1,2,4-trimethylbenzene and mesitylene can be used.

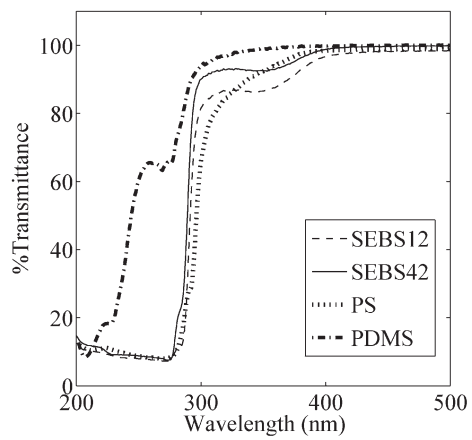

Fig. 5 UV-vis spectra of SEBS12, SEBS42, PS, and PDMS. All materials show transmittance near 100% down to approximately 400 nm (500–800 nm are not shown for clarity), with PDMS having improved transmittance below 350 nm. SEBS42 shows slightly higher transmittance than SEBS12 and PS from 300–350 nm.

Analysis of the surface composition indicates that substrate and bulk polymer choice effect the amount of PS at the surface of the microdevices. SEBS42 casted onto different substrates experienced increasing PS surface concentration on silane, SU-8, and silicon surfaces respectively. In terms of practical use, silane treated wafers offer the greatest durability, followed by the all SU-8 wafers, which allow for easier de-molding than untreated silicon, but degrade over time.

Contact angle measurements indicate that the surface of SEBS42 is marginally hydrophobic, but can be made hydrophilic following oxygen plasma treatment before undergoing moderate hydrophobic recovery over the course of a few days. The SEBS42 native, oxidized, and fibronectin treated surface are all biocompatible, supporting 3T3 and BPAEC cell attachment and proliferation. SEBS42 treated with FN shows cell growth that is generally comparable to standard tissue culture dishes. Other advantageous properties of SEBS42

Table 2 Summary of fabrication and material properties of PDMS, SEBS12, SEBS42, and PS. Number of plus signs (+) indicate relative strengths (more +) and weaknesses (less + or −) of materials

		PDMS	SEBS12	SEBS42	PS
Fabrication	Ease of demolding	++	++	++	−
	Bonding	+	++	++	−
	Interfacing	++	+	+	−
Material properties	Elastic modulus	1–3 MPa	~0.8 MPa	~6.2 MPa	3 GPa
	Advancing contact angle	108°	113°	95.9°	91–94°
	Surface stability	−	+	+	++
	PS surface content	−	2%	25%	100%
	Cell culture	++	NA	++	+++
	Zeta potential (pH 7)	−25–32 mV	NA	−39 mV	−20–30 mV
	Thermal stability	+	NA	+	−
	Molecule sorption	−	NA	++	++
	Optical transparency	++	+	+	+
	Autofluorescence	+	+	+	+

include high bonding strength, stable zeta potential, high optical transparency, low autofluorescence, little to no adsorption and absorption of small hydrophobic molecules, relatively high thermal stability, and rugged mechanical properties. The simple fabrication and material properties of SEBS42 make it a quality substrate for microfluidic applications.

Acknowledgements

The authors thank Dan Graham, Ph.D., for developing the NESAC/BIO Toolbox used in this study and NIH grant EB-002027 for supporting the toolbox development. The authors also thank Evgenia Yuferova for her efforts and contributions to the work.

Notes and references

1 A. Folch and M. Toner, *Annu. Rev. Biomed. Eng.*, 2000, **2**, 227–256.
2 D. J. Beebe, G. A. Mensing and G. M. Walker, *Annu. Rev. Biomed. Eng.*, 2002, **4**, 261–286.
3 T. M. Keenan and A. Folch, *Lab Chip*, 2008, **8**, 34.
4 E. W. K. Young and D. J. Beebe, *Chem. Soc. Rev.*, 2010, **39**, 1036.
5 A. R. Wheeler, W. R. Throndset, R. J. Whelan, A. M. Leach, R. N. Zare, Y. H. Liao, K. Farrell, I. D. Manger and A. Daridon, *Anal. Chem.*, 2003, **75**, 3581–3586.
6 P. Yager, T. Edwards, E. Fu, K. Helton, K. Nelson, M. R. Tam and B. H. Weigl, *Nature*, 2006, **442**, 412–418.
7 P. S. Dittrich and A. Manz, *Nat. Rev. Drug Discovery*, 2006, **5**, 210–218.
8 L. Kang, *Drug Discovery Today*, 2008, **13**, 1–13.
9 I. K. Zervantonakis, C. R. Kothapalli, S. Chung, R. Sudo and R. D. Kamm, *Biomicrofluidics*, 2011, **5**, 013406.
10 A. R. Wu, T. L. A. Kawahara, N. A. Rapicavoli, J. van Riggelen, E. H. Shroff, L. Xu, D. W. Felsher, H. Y. Chang and S. R. Quake, *Lab Chip*, 2012, **12**, 2190.
11 E. Berthier, E. W. K. Young and D. Beebe, *Lab Chip*, 2012, **12**, 1224.
12 A. S. Curtis, J. V. Forrester, C. McInnes and F. Lawrie, *J. Cell Biol.*, 1983, **97**, 1500–1506.
13 D. C. Duffy, J. C. McDonald, O. J. A. Schueller and G. M. Whitesides, *Anal. Chem.*, 1998, **70**, 4974–4984.
14 Y. Xia and G. M. Whitesides, *Annu. Rev. Mater. Sci.*, 1998, **28**, 153–184.
15 G. M. Whitesides, E. Ostuni, S. Takayama, X. Jiang and D. M. Ingber, *Annu. Rev. Biomed. Eng.*, 1992, **3**, 335–373.
16 H. Becker and U. Heim, *Sens. Actuators, A*, 2000, **83**, 130–135.
17 G. S. Fiorini and D. T. Chiu, *et al.*, *BioTechniques*, 2005, **38**, 429.
18 U. M. Attia, *Microfluid. Nanofluid.*, 2009, **7**, 1–28.
19 G. Mehta, J. Lee, W. Cha, Y.-C. Tung, J. J. Linderman and S. Takayama, *Anal. Chem.*, 2009, **81**, 3714–3722.
20 Y. Wang, J. Balowski, C. Phillips, R. Phillips, C. E. Sims and N. L. Allbritton, *Lab Chip*, 2011, **11**, 3089.
21 C.-W. Tsao and D. L. DeVoe, *Microfluid. Nanofluid.*, 2008, **6**, 1–16.
22 M. W. Toepke and D. J. Beebe, *Lab Chip*, 2006, **6**, 1484.
23 K. J. Regehr, M. Domenech, J. T. Koepsel, K. C. Carver, S. J. Ellison-Zelski, W. L. Murphy, L. A. Schuler, E. T. Alarid and D. J. Beebe, *Lab Chip*, 2009, **9**, 2132.
24 X. Su, E. W. K. Young, H. A. S. Underkofler, T. J. Kamp, C. T. January and D. J. Beebe, *J. Biomol. Screening*, 2010, **16**, 101–111.
25 J. D. Wang, N. J. Douville, S. Takayama and M. ElSayed, *Ann. Biomed. Eng.*, 2012, **40**, 1862–1873.
26 H. Shiku, T. Saito, C. Wu, T. Yasukawa, M. Yokoo, H. Abe, T. Matsue and H. Yamada, *Chem. Lett.*, 2006, **35**, 234.
27 J. Kuncová-Kallio and P. J. Kallio, in *Engineering in Medicine and Biology Society, 2006. EMBS'06. 28th Annual International Conference of the IEEE*, 2006, pp. 2486–2489.
28 H. Makamba, J. H. Kim, K. Lim, N. Park and J. H. Hahn, *Electrophoresis*, 2003, **24**, 3607–3619.
29 M. Morra, E. Occhiello, F. Garbassi, M. Maestri, R. Bianchi and A. Zonta, *Clin. Mater.*, 1990, **5**, 147–156.
30 J. S. Gewandter, R. J. Staversky and M. A. O'Reilly, *Free Radical Biol. Med.*, 2009, **47**, 1742–1752.
31 Y. S. Heo, L. M. Cabrera, J. W. Song, N. Futai, Y. C. Tung, G. D. Smith and S. Takayama, *Anal. Chem.*, 2007, **79**, 1126–1134.

32 G. M. Walker, H. C. Zeringue and D. J. Beebe, *Lab Chip*, 2004, **4**, 91–97.
33 S. Hu, X. Ren, M. Bachman, C. E. Sims, G. P. Li and N. Allbritton, *Anal. Chem.*, 2002, **74**, 4117–4123.
34 G. T. Roman and C. T. Culbertson, *Langmuir*, 2006, **22**, 4445–4451.
35 J. Zhou, A. V. Ellis and N. H. Voelcker, *Electrophoresis*, 2009, **31**, 2–16.
36 M. D. Guillemette, E. Roy, F. A. Auger and T. Veres, *Acta Biomater.*, 2011, **7**, 2492–2498.
37 A. P. Sudarsan, J. Wang and V. M. Ugaz, *Anal. Chem.*, 2005, **77**, 5167–5173.
38 E. Roy, M. Geissler, J.-C. Galas and T. Veres, *Microfluid. Nanofluid.*, 2011, **11**, 235–244.
39 E. Roy, J.-C. Galas and T. Veres, *Lab Chip*, 2011, **11**, 3193.
40 D. Brassard, L. Clime, K. Li, M. Geissler, C. Miville-Godin, E. Roy and T. Veres, *Lab Chip*, 2011, **11**, 4099.
41 N. J. Sniadecki and C. S. Chen, *Methods Cell Biol.*, 2007, **83**, 313–328.
42 A. Sze, D. Erickson, L. Ren and D. Li, *J. Colloid Interface Sci.*, 2003, **261**, 402–410.
43 E. Sollier, C. Murray, P. Maoddi and D. Di Carlo, *Lab Chip*, 2011, **11**, 3752–3765.
44 J. C. McDonald and G. M. Whitesides, *Acc. Chem. Res.*, 2002, **35**, 491–499.
45 E. Delamarche, H. Schmid, B. Michel and H. Biebuyck, *Adv. Mater.*, 2004, **9**, 741–746.
46 B. Michel, A. Bernard, A. Bietsch, E. Delamarche, M. Geissler, D. Juncker, H. Kind, J. P. Renault, H. Rothuizen and H. Schmid, *IBM J. Res. Dev.*, 2001, **45**, 697–719.
47 H. Schmid and B. Michel, *Macromolecules*, 2000, **33**, 3042–3049.
48 Kraton Polymer, *SEBS A1536H Copolymer Material Data Sheet*.
49 Y. Agari, A. Ueda and S. Nagai, *J. Appl. Polym. Sci.*, 1993, **47**, 331–335.
50 Y. Agari, A. Ueda and S. Nagai, *J. Appl. Polym. Sci.*, 1992, **45**, 1957–1961.
51 G. H. Fredrickson, *Macromolecules*, 1987, **20**, 2535–2542.
52 T. P. Russell, G. Coulon, V. R. Deline and D. C. Miller, *Macromolecules*, 1989, **22**, 4600–4606.
53 R. A. Segalman, *Mater. Sci. Eng., R*, 2005, **48**, 191–226.
54 J. N. L. Albert and T. H. Epps, *Mater. Today*, 2010, **13**, 24–33.
55 P. Mansky, T. P. Russell, C. J. Hawker, J. Mays, D. C. Cook and S. K. Satija, *Phys. Rev. Lett.*, 1997, **79**, 237–240.
56 G. Chauve, L. Heux, R. Arouini and K. Mazeau, *Biomacromolecules*, 2005, **6**, 2025–2031.
57 Y. Li, H. Liu, J. Song, O. J. Rojas and J. P. Hinestroza, *ACS Appl. Mater. Interfaces*, 2011, **3**, 2349–2357.
58 C. S. Henkee, E. L. Thomas and L. J. Fetters, *J. Mater. Sci.*, 1988, **23**, 1685–1694.
59 D. J. Graham and D. G. Castner, *Biointerphases*, 2012, **7**, 1–12.
60 D. J. Graham and B. D. Ratner, *Langmuir*, 2002, **18**, 5861–5868.
61 M. S. Wagner and D. G. Castner, *Langmuir*, 2001, **17**, 4649–4660.
62 L. T. Weng, P. Betrand, W. Lauer, R. Zimmer and S. Busetti, *Surf. Interface Anal.*, 1995, **23**, 879–886.
63 S. Liu, L.-T. Weng, C.-M. Chan, L. Li, N. K. Ho and M. Jiang, *Surf. Interface Anal.*, 2001, **31**, 745–753.
64 S. Liu, C.-M. Chan, L.-T. Weng and M. Jiang, *Anal. Chem.*, 2004, **76**, 5165–5171.
65 I. Beaulieu, M. Geissler and J. Mauzeroll, *Langmuir*, 2009, **25**, 7169–7176.
66 G. Altankov and T. Groth, *J. Biomater. Sci., Polym. Ed.*, 1997, **8**, 299–310.
67 T. G. van Kooten, H. T. Spijker and H. J. Busscher, *Biomaterials*, 2004, **25**, 1735–1747.
68 B. J. Kirby and E. F. Hasselbrink, *Electrophoresis*, 2004, **25**, 187–202.
69 B. J. Kirby and E. F. Hasselbrink, *Electrophoresis*, 2004, **25**, 203–213.
70 J. N. Lee, X. Jiang, D. Ryan and G. M. Whitesides, *Langmuir*, 2004, **20**, 11684–11691.
71 H. Sasaki, H. Onoe, T. Osaki, R. Kawano and S. Takeuchi, *Sens. Actuators, B*, 2010, **150**, 478–482.
72 K. Ren, Y. Zhao, J. Su, D. Ryan and H. Wu, *Anal. Chem.*, 2010, **82**, 5965–5971.
73 R. Gomez-Sjoberg, A. A. Leyrat, B. T. Houseman, K. Shokat and S. R. Quake, *Anal. Chem.*, 2010, **82**, 8954–8960.
74 A. L. Garcia, L. K. Ista, D. N. Petsev, M. J. O'Brien, P. Bisong, A. A. Mammoli, S. R. J. Brueck and G. P. López, *Lab Chip*, 2005, **5**, 1271.

